Resolving Complex Atomic-Scale Spin Structures by Spin-Polarized Scanning Tunneling Microscopy

D. Wortmann,[1] S. Heinze,[1,2] Ph. Kurz,[1] G. Bihlmayer,[1] and S. Blügel[1,*]

[1]*Institut für Festkörperforschung, Forschungszentrum Jülich, D-52425 Jülich, Germany*

[2]*Institute of Applied Physics and Microstructure Research Center, University of Hamburg, Jungiusstrasse 11, D-20355 Hamburg, Germany*

(Received 7 August 2000)

The spin-polarized scanning tunneling microscope (SP-STM) operated in the constant current mode is proposed as a powerful tool to investigate complex atomic-scale magnetic structures of otherwise chemically equivalent atoms. The potential of this approach is demonstrated by successfully resolving the magnetic structure of Cr/Ag(111), which is predicted on the basis of *ab initio* vector spin-density calculations to be a coplanar noncollinear periodic 120° Néel structure. Different operating modes of the SP-STM are discussed on the basis of the model of Tersoff and Hamann.

DOI: 10.1103/PhysRevLett.86.4132 PACS numbers: 75.30.Fv, 68.37.Ef, 75.70.Ak, 75.70.Rf

Exploiting the spin, rather than the charge degrees of freedom, is the core vision behind the current excitement driving the rapid developments in magneto- and spin electronics. Some of the key issues relate to the understanding of the magnetic properties of nanoscale magnets with competing exchange interactions between neighboring atoms. Examples are (ultrathin) ferromagnetic films in contact with antiferromagnetic ones, as is common for exchange-bias systems [1] used in the magnetic recording industry. In many cases, the geometrical arrangement of the atoms does not allow one to satisfy the competing exchange interactions between neighboring atoms, which leads to frustrated spin structures. Frustration gives rise to a wide variety of complex spin structures on the atomic scale, such as antiferromagnetism, spiral spin-density waves (SSDW), or general noncollinear states [2]. These spin structures are still poorly understood because of the inability of traditional techniques to spatially determine the magnetic structure. Even the currently most advanced techniques, the x-ray spectromicroscopy [3] and the spin polarized scanning tunneling microscope (SP-STM) in the spectroscopy mode [4,5], have no atomic-scale resolution.

In this paper we introduce a new powerful method — the SP-STM operated in the constant current mode — to image complex magnetic structures at surfaces on the atomic scale. By applying the Tersoff-Hamann model [6] to the case of a SP-STM and considering the effect of the vacuum barrier on the lateral resolution of the STM, we show that in general the SP-STM image of any periodic magnetic superstructure of otherwise chemically equivalent atoms displays a pronounced pattern corresponding to the magnetic configuration and not to the geometric arrangement of the atoms. This is in contradiction to the conventional wisdom that spin polarization is a small effect and that therefore the nonspin-polarized STM image reflecting the atomic structure will be only slightly modulated in the SP-STM experiment.

This approach opens up a new route for using the STM, namely, besides the exploration of the topological, chemical, and ferromagnetic structure of surfaces, and also the inherently much more difficult investigation of surfaces with noncollinear spin structures with ultimate, i.e., atomic, resolution. This new concept was very recently applied for the first time to prove experimentally [7] the existence of antiferromagnetism in two dimensions (2D), predicted [8] more than ten years ago. Here, we extend the applicability to arbitrary spin-structures. The potential of the SP-STM in the constant current mode is demonstrated by successfully resolving the magnetic structure of one monolayer (ML) Cr on Ag(111). On the basis of first-principles total energy calculations the magnetic ground state of one Cr monolayer on Ag(111) is predicted to be a 2D noncollinear periodic 120° Néel structure.

The working principle of the SP-STM is the tunneling of spin-polarized electrons between tip and sample across the vacuum barrier. It can be realized by coating a common STM tip with various magnetic materials, e.g., Fe or Gd [4,9], and using these spin-sensitive probes to scan the surface of the magnetic sample. In the following we assume the coated tip to be ferromagnetic with a spin-polarized electronic structure of spin-up (↑) and spin-down (↓) states with respect to the quantization axis given by the magnetization axis $\hat{\mathbf{e}}_M^T$ of the tip.

According to Bardeen's [10] description of tunneling, the tunneling current I as a function of the bias voltage V and the position of the tip $\mathbf{R}_T$ is written in the nonspin-polarized case as

$$I(\mathbf{R}_T, V) = \frac{2\pi e}{\hbar} \sum_{\mu,\nu} [f(\epsilon_\mu^S - \epsilon_F) - f(\epsilon_\nu^T - \epsilon_F)] \times \delta(\epsilon_\nu^T - \epsilon_\mu^S - eV) |M_{\nu,\mu}(\mathbf{R}_T)|^2, \quad (1)$$

where $f(\epsilon)$ is the Fermi function, $\epsilon_{\mu/\nu}^{T/S}$ are the energies of the tip/sample states, and ϵ_F is the Fermi energy. The key problem is to calculate the matrix elements given by

$$M_{\nu,\mu}(\mathbf{R}_T) = \langle \Psi_\nu^T | U_T | \Psi_\mu^S \rangle, \quad (2)$$

where U_T denotes the potential of the tip.

 0031-9007/01/86(18)/4132(4)$15.00

To extend the description to the spin-polarized case, Eq. (2) is rewritten in a more general form using the two component spinors for the wave functions. For a ferromagnetic tip, the spinor of the tip–wave function can be written in terms of a pure spin-state:

$$\Psi_\nu^T = \begin{pmatrix} \psi_{\nu\uparrow}^T \\ 0 \end{pmatrix} \quad \text{or} \quad \Psi_\nu^T = \begin{pmatrix} 0 \\ \psi_{\nu\downarrow}^T \end{pmatrix}. \tag{3}$$

The sample, on the other hand, may possess a variety of different magnetic structures. In general, the wave functions of the sample Ψ_μ^S are spin mixed. This is evidently true for noncollinear systems since no quantization axis exists which allows a state to be written in terms of pure spin-up or spin-down character, but even for collinear samples the states will be spin mixed if the quantization axis of the sample and the tip is not aligned in parallel. Thus, by using for both tip and sample the quantization axis of the tip, the state of the sample will be of the general form

$$\Psi_\mu^S = \begin{pmatrix} \psi_{\mu\uparrow}^S \\ \psi_{\mu\downarrow}^S \end{pmatrix}. \tag{4}$$

Assuming spin conserving tunneling across the vacuum barrier, i.e., ignoring spin-flip processes, e.g., due to the spin-orbit interaction or defects, the tip potential $\mathbf{U}_T$ is diagonal in spin space, and the spin-dependent matrix element can be written as

$$M_{\nu,\mu}^\sigma(\mathbf{R}_T) = \langle \psi_{\nu\sigma}^T | U_{T\sigma\sigma} | \psi_{\mu\sigma}^S \rangle = -\frac{2\pi C\hbar^2}{\kappa m}\, \psi_{\mu\sigma}^S(\mathbf{R}_T), \tag{5}$$

where $\sigma = \uparrow, \downarrow$ denotes the spin index. The right-hand side of Eq. (5) can be derived following Tersoff and Hamann [6] by replacing the wave function at the tip apex atom by a spherically symmetric s wave. We assume that the spin-up and spin-down s-wave states can be characterized by the same decay constant κ and the same normalization coefficient C. In analogy to the model of Tersoff and Hamann we further assume that the spin-up, $n_T^\uparrow(\epsilon)$, and spin-down, $n_T^\downarrow(\epsilon)$, tip density of states (DOS) are constant in energy but different in size to account for the magnetization of the tip, $\mathbf{m}_T = (n_T^\uparrow - n_T^\downarrow)\mathbf{e}_M^T$. Inserting the matrix elements into Eq. (1) leads to

$$I(\mathbf{R}_T, V, \theta) = \frac{8\pi^3 C^2 \hbar^3 e}{\kappa^2 m^2} \int d\epsilon\, g_V(\epsilon) \sum_\mu \delta(\epsilon_\mu - \epsilon) \times [n_T^\uparrow |\psi_{\mu\uparrow}^S(\mathbf{R}_T)|^2 + n_T^\downarrow |\psi_{\mu\downarrow}^S(\mathbf{R}_T)|^2], \tag{6}$$

with $g_V(\epsilon) = f(\epsilon - \epsilon_F) - f(\epsilon + eV - \epsilon_F)$. $\theta(\mathbf{R}_T, V)$ denotes the angle between the magnetization direction of the tip and the sample at $\mathbf{R}_T$ and depends on the degree of spin mixing of all states μ within the energy interval between ϵ_F and $\epsilon_F + eV$. For a collinear orientation ($\theta = 0°, \theta = 180°$) of the tip and sample magnetization, Eq. (6) can be understood as a trivial generalization of the standard, nonspin-polarized expression of Tersoff and Hamann. For a general magnetic structure, however, the situation is more complicated as $|\psi_{\mu\downarrow/\uparrow}^S(\mathbf{R}_T)|^2$ can no longer simply be interpreted as a local DOS (LDOS). In this case it is instructive to write the current as

$$I(\mathbf{R}_T, V, \theta) = I_0(\mathbf{R}_T, V) + I_P(\mathbf{R}_T, V, \theta), \tag{7}$$

$$= \frac{4\pi^3 C^2 \hbar^3 e}{\kappa^2 m^2} [n_T \tilde{n}_S(\mathbf{R}_T, V) + \mathbf{m}_T \tilde{\mathbf{m}}_S(\mathbf{R}_T, V)]. \tag{8}$$

We have introduced the integrated LDOS (ILDOS) $\tilde{n}_S(\mathbf{R}_T, V)$ and the vector of the integrated local magnetization DOS $\tilde{\mathbf{m}}_S(\mathbf{R}_T, V)$ of the sample. The latter is given by an energy integral of the local magnetization DOS, $\mathbf{m}_S(\mathbf{R}_T, \epsilon)$:

$$\mathbf{m}_S(\mathbf{R}_T, \epsilon) = \sum_\mu \delta(\epsilon_\mu - \epsilon) \Psi_\mu^{S\dagger}(\mathbf{R}_T) \boldsymbol{\sigma} \Psi_\mu^S(\mathbf{R}_T), \tag{9}$$

$$\tilde{\mathbf{m}}_S(\mathbf{R}_T, V) = \int d\epsilon\, g_V(\epsilon) \mathbf{m}_S(\mathbf{R}_T, \epsilon). \tag{10}$$

Analogously, the LDOS and the ILDOS of the sample $n_S(\mathbf{R}_T, \epsilon)$ and $\tilde{n}_S(\mathbf{R}_T, V)$ are defined by Eqs. (9) and (10), replacing Pauli's spin matrix $\boldsymbol{\sigma}$ by the unit matrix. Equations (7) and (8) state that the tunneling current can be separated into an unpolarized part I_0 depending on the ILDOS of the sample at the position of the tip and a spin-polarized contribution I_P given by the projection of the vector of the integrated local magnetization DOS of the sample onto the magnetization direction of the tip. In the case of a nonspin-polarized STM experiment, i.e., using either a nonmagnetic tip or sample, the second term vanishes and the current reduces to the result of the Tersoff-Hamann model.

The main objective in obtaining a magnetic contrast in the SP-STM image is to decouple I_P from I_0. The SP-STM experiments reported recently, such as the investigation of the dipolar antiferromagnetism of Fe nanowires on W(110) [4], the topological antiferromagnetism of Cr(001) [5], or the magnetic domains of thin films [11], were not carried out in the constant current, but in the spin-polarized scanning tunneling spectroscopy mode, i.e., a map of the differential conductivity dI/dV,

$$\frac{dI}{dV}(\mathbf{R}_T, V) \propto n_T n_S(\mathbf{R}_T, \epsilon_F + eV) + \mathbf{m}_T \mathbf{m}_S(\mathbf{R}_T, \epsilon_F + eV), \tag{11}$$

at a well-chosen bias voltage V is correlated with the topography of the sample. Comparing Eq. (11) with Eq. (8) reveals the essential difference between the contrast mechanisms of the two operating modes. While the differential conductivity is directly proportional to n_S and $\mathbf{m}_S$ at the energy $\epsilon_F + eV$, which is chosen such as to maximize the value of m_s over n_S, the constant current STM image, given by the vertical adjustment $\Delta z(\mathbf{r}_\parallel, V, \theta)$ of the tip to constant tunneling current I, is governed by the energy integrated quantities $\tilde{n}_S$ and $\tilde{\mathbf{m}}_S$. $\tilde{n}_S$ or I_0 always increases with the bias voltage V,

while $\tilde{\mathbf{m}}_S$ or I_P may stay constant. Thus the constant current mode of the SP-STM provides little magnetic contrast between different magnetic domains since I_0 dominates the tunneling current. This makes an imaging of alternating magnetization directions across domains using the constant current mode [12] extremely difficult.

A different solution used to decouple I_0 from I_P was recently introduced to investigate magnetic domains at a ferromagnetic surface [13]. By using a different tip setup, the magnetization of the tip was dynamically modulated at high frequency. According to Eq. (8) this leads to a signal given by the differential magnetic conductivity $dI/dm_T \propto \tilde{m}_S$. Thus, both the spectroscopy and the modulated tip magnetization mode have already shown their potential in resolving nanoscale spin structures, in accordance with Eq. (8). However, their resolution seems limited to about 1 nm. Thus they are inapplicable to reveal complex atomic-scale spin structures. Surprisingly, the simple constant current mode, as we will now show, is capable of providing this ultimate magnetic resolution.

The constant current image, $\Delta z(\mathbf{r}_\parallel, V, \theta)$, is determined by the change ΔI of the tunneling current. For a surface with 2D translational symmetry, ΔI can be written in terms of a 2D Fourier expansion:

$$\Delta I(\mathbf{r}_\parallel, z, V, \theta) = \sum_{n \neq 0} \Delta I_{\mathbf{G}_\parallel^n}(z, V, \theta) e^{i\mathbf{G}_\parallel^n \mathbf{r}_\parallel}, \qquad (12)$$

where $\mathbf{G}_\parallel^n$ denotes the reciprocal lattice vectors parallel to the surface, and $\Delta I_{\mathbf{G}_\parallel^n}(z, V, \theta)$ is the tip-sample distance (z) dependent expansion coefficient. This expansion can be applied to the unpolarized part of the current, I_0, as well as to the spin-polarized part, I_P, of Eq. (7). The expansion coefficients decay exponentially with increasing length of $\mathbf{G}_\parallel^n$ [14] and hence the STM image is dominated to a good approximation by the smallest nonvanishing reciprocal lattice vector $\mathbf{G}_\parallel^{(1)}$:

$$\Delta I_{\mathbf{G}_\parallel^{(1)}}(z, V, \theta) \propto e^{-2z\sqrt{2m/\hbar^2|\epsilon_F + eV| + (G_\parallel^{(1)}/2)^2}}. \qquad (13)$$

Any magnetic superstructure lowers the translational symmetry. Therefore, smaller reciprocal lattice vectors become relevant for the spin-polarized part of the tunneling current, I_P, with coefficients which are consequently exponentially larger than those of the unpolarized part, I_0. A constant current SP-STM image thus reflects the magnetic superstructure rather than the atomic or chemical unit cell even in the case of small effective spin polarization, for example, if the angle θ is close to 90°. A first experimental verification of this imaging mechanism was very recently given by the investigation of 2D antiferromagnetism at surfaces [7].

Even though we expect the magnetic signal to be strong due to different decay lengths, the electronic structure, contained in $\Delta I_{\mathbf{G}_\parallel^n}$, of a specific surface can still compete with this effect favoring the contribution of the lowest $\mathbf{G}_\parallel$ vector, and hence first-principles calculations need to be performed in order to interpret the experiments unambiguously. On the basis of such calculations we now propose to investigate the complex spin structure of 1 ML Cr on Ag(111) by SP-STM. The nearest neighbor exchange interaction of Cr is antiferromagnetic [8] and the Ag(111) substrate provides a triangular lattice, thus, we expect a frustrated spin structure. We investigate the ground-state spin structure of 1 ML Cr on Ag(111) by performing self-consistent *ab initio* calculations based on the density-functional theory in the local spin-density approximation [15]. We apply the full-potential linearized augmented plane-wave method in film geometry [16] as implemented in the program FLEUR recently extended [17] to treat noncollinear magnetic structures such as SSDWs [18].

We calculate the total energy $E(\mathbf{Q}_\parallel)$ and the magnetic moments $M(\mathbf{Q}_\parallel)$ of the SSDW for a discrete set of wave vectors $\mathbf{Q}_\parallel$ along the high-symmetry lines of a 2D Brillouin zone (BZ). This path includes all important magnetic high-symmetry states such as the ferromagnetic (FM) state, the row-wise antiferromagnetic (RW-AFM) state [a unit cell of two atoms, which are ferromagnetically aligned along a row of nearest neighbor atoms and antiferromagnetically aligned from row to row (see Fig. 1)], and the 120° Néel state [a 2D noncollinear structure with three atoms per surface unit cell, which consists of spins forming 120° angles between nearest neighbors (see Fig. 2)]. The calculations are carried out in a $p(1 \times 1)$ unit cell, taking 256 $\mathbf{k}_\parallel$-points in the full 2D BZ into account. The system is modeled by 1 ML of Cr on a substrate of four layers of Ag. The equilibrium interlayer distance between Cr and Ag was determined for the FM state by force calculations. We found that the Néel state has the lowest energy of all considered magnetic structures and is the magnetic ground state. It is 312 meV/atom lower in energy than FM and 39 meV/atom lower in energy than the RW-AFM state.

We now present the predicted STM images for both the RW-AFM structure and the 120° Néel state. Figure 1 shows the calculated STM images for the RW-AFM structure. Figure 1(a) shows an image calculated for a

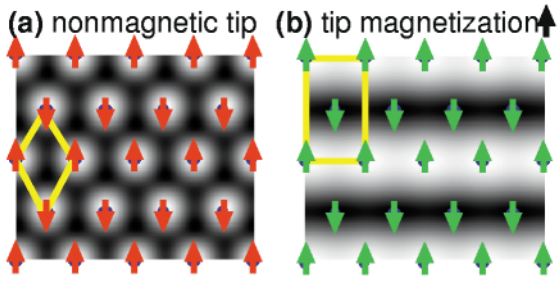

FIG. 1 (color). Calculated STM images for the RW-AFM structure at a bias voltage of −0.5 V for a tip-sample distance of 3.7 Å and a fully spin-polarized tip [19]. The left (right) panel shows the image calculated for a nonmagnetic (magnetic) STM tip. The structure of the unit cell (yellow), the directions of the magnetic moments (red), and its projection on the direction of the moment of the tip (green) are superimposed.

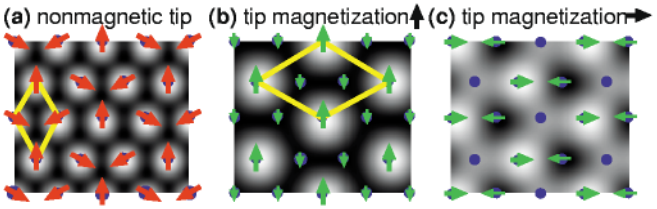

FIG. 2 (color). Calculated STM images for the Néel structure. The image for conventional STM (nonmagnetic tip) and for two different directions of the tip magnetization, i.e., for two different values of θ, are displayed.

nonmagnetic STM tip resulting in a hexagonal pattern corresponding to the chemical unit cell. Figure 1(b), on the other hand, displays the SP-STM image calculated for a magnetic tip with a magnetization axis parallel to the one of the sample. We find a stripe pattern reflecting the broken symmetry between the atoms of different rows. Atoms with a magnetic moment parallel to the magnetization of the tip are imaged as protrusions while atoms with antiparallel magnetic moments appear as depressions. This setup provides maximal magnetic contrast ($\Delta z \approx 0.2$ Å for a tip with a spin polarization of 40% [7,9]) as the angle between the direction of the magnetization of the tip and the magnetization of the sample is zero. A different angle would simply lead to a reduction of the magnetic contrast, even restoring Fig. 1(a) for $\theta \rightarrow 90°$.

Now we turn to the Néel structure displayed in Fig. 2. Again, Fig. 2(a) shows the STM image as expected for an unpolarized tip which is of course the same as the one shown in Fig. 1(a). The other two plots [Figs. 2(b) and 2(c)] correspond to SP-STM images calculated for magnetic tips with two different directions of the magnetization. For Fig. 2(b) the magnetization of the tip has been chosen parallel to the magnetic moment of one of the three magnetically inequivalent atoms, while the projection of the magnetic moment of the two other atoms onto the tip magnetization is the same. Consequently, the image displays a $(\sqrt{3} \times \sqrt{3})$ superstructure ($\Delta z \approx 0.1$ Å). If the projected magnetization, $\tilde{\mathbf{m}}_S \mathbf{e}_M^T$, is different for all atoms in a surface unit cell as in Fig. 2(c), additional features appear in the image and the contrast is reduced. We conclude that not only the magnitude of the magnetic contrast but also the pattern of the SP-STM image depends on the direction of the magnetization of the tip for the 120° Néel structure. While it is not clear whether the images as shown in Figs. 2(b) and 2(c) could be distinguished in a real experiment, it is obvious that the RW-AFM and the Néel state can be easily distinguished, depending on whether a stripe pattern or a $(\sqrt{3} \times \sqrt{3})$ superstructure will be found.

We discussed the constant current, the spectroscopy, and the modulated tip magnetization mode of a SP-STM probing a magnetic surface with an arbitrary magnetic structure. On the basis of the spin dependent Tersoff-Hamann model we propose the investigation of complex atomic-scale magnetic structures at surfaces using a SP-STM operated in the constant current mode. The SP-STM image will correspond to the magnetic superstructure and not to the atomic or chemical unit cell. To demonstrate this concept we calculated SP-STM images of a monolayer Cr on Ag(111). Based on total-energy calculations, we predict that the magnetic ground state is a 120° periodic Néel state. We conclude that the SP-STM allows a clear distinction between the proposed 120° Néel state and the competing RW-AFM or FM state. Very likely this concept can be carried over to image magnetic interfaces buried below surfaces of metals with strongly dispersive electron states. As pointed out by Wortmann *et al.* [20] quantum-well states between the surface and the interface will develop which will mediate the information of the interface to the surface.

S. H. thanks O. Pietzsch, A. Kubetzka, Dr. M. Bode, and Professor R. Wiesendanger for many fruitful discussions. This work was supported by the DFG under Grants No. BL 444/1 and No. Wi 1277/6, and the TMR Network, Contract No. FMRX-CT98-0178.

*Electronic address: s.bluegel@fz-juelich.de

[1] J. Nogues and I. K. Schuller, J. Magn. Magn. Mater. **192**, 203 (1999).
[2] Directions of magnetic moments at different atom sites are not aligned along a global quantization axis.
[3] A. Scholl *et al.,* Science **287**, 1014 (2000).
[4] O. Pietzsch, A. Kubetzka, M. Bode, and R. Wiesendanger, Phys. Rev. Lett. **84**, 5212 (2000).
[5] M. Kleiber *et al.,* Phys. Rev. Lett. **85**, 4606 (2000).
[6] J. Tersoff and D. Hamann, Phys. Rev. Lett. **50**, 1998 (1983).
[7] S. Heinze *et al.,* Science **288**, 1805 (2000).
[8] S. Blügel, M. Weinert, and P. H. Dederichs, Phys. Rev. Lett. **60**, 1077 (1988).
[9] M. Bode, M. Getzlaff, and R. Wiesendanger, J. Vac. Sci. Technol. A **17**, 2228 (1999).
[10] J. Bardeen, Phys. Rev. Lett. **6**, 57 (1961).
[11] M. Bode, M. Getzlaff, and R. Wiesendanger, Phys. Rev. Lett. **81**, 4256 (1998).
[12] R. Wiesendanger *et al.,* Phys. Rev. Lett. **65**, 247 (1990).
[13] W. Wulfhekel and J. Kirschner, Appl. Phys. Lett. **75**, 1944 (1999).
[14] S. Heinze *et al.,* Phys. Rev. B **58**, 16 432 (1998).
[15] V. L. Moruzzi, J. F. Janak, and A. R. Williams, *Calculated Electronic Properties of Metals* (Pergamon, New York, 1978).
[16] E. Wimmer *et al.,* Phys. Rev. B **24**, 864 (1981); M. Weinert *et al.,* Phys. Rev. B **26**, 4571 (1982).
[17] Ph. Kurz, G. Bihlmayer, and S. Blügel, J. Appl. Phys. **87**, 6101 (2000).
[18] L. Nordström and A. Mavromaras, Europhys. Lett. **49**, 775 (2000).
[19] We found no qualitative dependence of the STM images on the bias voltage or the tip-sample distance ($z \geq 3$ Å).
[20] D. Wortmann, S. Heinze, G. Bihlmayer, and S. Blügel (to be published).